

Plasmon polaritons in 1D Cantor-like fractal photonic superlattices containing a left-handed material

This content has been downloaded from IOPscience. Please scroll down to see the full text.

2011 EPL 95 24004

(<http://iopscience.iop.org/0295-5075/95/2/24004>)

View [the table of contents for this issue](#), or go to the [journal homepage](#) for more

Download details:

IP Address: 200.24.16.226

This content was downloaded on 17/01/2017 at 21:40

Please note that [terms and conditions apply](#).

You may also be interested in:

[Plasmon polaritons in photonic superlattices containing a left-handed material](#)

E. Reyes-Gómez, D. Mogilevtsev, S. B. Cavalcanti et al.

[Zero-angle n angle non-Bragg gap plasmon-polariton modes and omni-reflectance in 1Dmetamaterial photonic superlattices](#)

C Agudelo-Arango, J R Mejía-Salazar, N Porrás-Montenegro et al.

[Absorption effects on plasmon polaritons in quasiperiodic photonic superlattices containing a metamaterial](#)

E Reyes-Gómez, N Raigoza, S B Cavalcanti et al.

[Field profiles of bulk plasmon polariton modes in layered systems containing a metamaterial](#)

A Bruno-Alfonso, E Reyes-Gómez, S B Cavalcanti et al.

[Omnidirectional suppression of Anderson localization of light in disordered one-dimensional photonic superlattices](#)

E Reyes-Gómez, S B Cavalcanti and L E Oliveira

[Exploiting aperiodic designs in nanophotonic devices](#)

Enrique Maciá

[Optical transmission spectra in quasiperiodic multilayered photonic structure](#)

F F de Medeiros, E L Albuquerque and M S Vasconcelos

[Nonlinear photonic crystal: effects of negative refractive indices and dispersion in the resonant region](#)

C H Raymond Ooi and Choo Yong Lee

Plasmon polaritons in 1D Cantor-like fractal photonic superlattices containing a left-handed material

J. R. MEJÍA-SALAZAR¹, N. PORRAS-MONTENEGRO¹, E. REYES-GÓMEZ^{2(a)}, S. B. CAVALCANTI³
and L. E. OLIVEIRA⁴

¹ *Departamento de Física, Universidad del Valle - AA 25360, Cali, Colombia*

² *Instituto de Física, Universidad de Antioquia - AA 1226, Medellín, Colombia*

³ *Instituto de Física, UFAL, Cidade Universitária - Maceió-AL, 57072-970, Brazil*

⁴ *Instituto de Física, UNICAMP - Campinas-SP, 13083-859, Brazil*

received 17 February 2011; accepted in final form 5 June 2011

published online 4 July 2011

PACS 41.20.Jb – Electromagnetic wave propagation; radiowave propagation

PACS 42.70.Gi – Light-sensitive materials

PACS 42.70.Qs – Photonic bandgap materials

Abstract – The propagation of light incident upon a 1D photonic superlattice consisting of successive stacking of alternate layers of a right-handed nondispersive material and a metamaterial, arranged to form a Cantor-like fractal, is considered. Plasmon-polariton excitations are thoroughly investigated within the transfer-matrix approach and shown to strongly depend on the Cantor step number N . More specifically, the number of plasmon-polariton bands corresponds to the number $2^N - 1$ of metamaterial layers within the unit cell.

Copyright © EPLA, 2011

Current progress in microstructuring techniques of high-quality optical materials available nowadays yields remarkable flexibility in the fabrication of nanostructures, which allows the realization of structures [1] with simultaneous negative permittivity ϵ and negative permeability μ and, hence, a negative refractive index $n = \sqrt{\epsilon\mu}$. Such negative refractive-index materials, also called left-handed materials or metamaterials, have been idealized by Veselago [2] who predicted unusual properties such as backward wave propagation and negative refraction. Moreover, metamaterials based on anisotropic semiconductors heterostructures have been realized, opening up new perspectives in the design and development of metamaterials and new optical semiconductor devices [3]. Recently, the study of the propagation of light through periodic multilayered photonic systems composed by alternating layers of right- and left-handed materials [4–7] have evidenced the existence of non-Bragg gaps insensitive to scale changes of the system, in contrast to the usual behavior exhibited by Bragg gaps. Also, Li *et al.* [8] have performed a theoretical study of the zero- $\langle n \rangle$ gap in the photonic spectra of quasiperiodic Fibonacci structures. Moreover, recent work has been focused on the excitation of bulk (electric) magnetic plasmon-polariton modes via the nonvanishing component of the (electric)

magnetic field along the growth direction of the photonic metamaterial heterostructure, and thoroughly examined the plasmon-polariton spectra in both periodic and quasiperiodic Fibonacci- and Thue-Morse-like photonic crystals [9–11].

The present work is concerned with the study of plasmon polaritons in 1D Cantor-like photonic superlattices composed by alternate layers of right- and dispersive left-handed materials. Nonperiodic multilayered structures generated in a way similar to the Cantor set [12–14] are termed as Cantor-like structures, which consist in fractal nonperiodic multilayer systems. Here we study a 1D Cantor-like photonic structure as depicted in fig. 1. One takes the seed to be a bulk of positive-refractive-index material (labeled A). The unitary cell of the photonic crystal is generated by substituting the middle third of the original seed by a dispersive refractive-index metamaterial (labeled B) as in step $N = 1$ of fig. 1. Step $N = 2$ corresponds to again substituting by metamaterials the middle third of the two remaining segments of positive-refractive-index material, as in $N = 2$ of fig. 1. The middle third of each remaining four segments are then substituted by metamaterials (step $N = 3$ of fig. 1), and so on to infinity.

Here we will be concerned with the propagation of an electromagnetic wave in 1D Cantor-like fractal photonic periodic superlattices with unit cell given by the N -th

^(a)E-mail: ereyesgomez@gmail.com

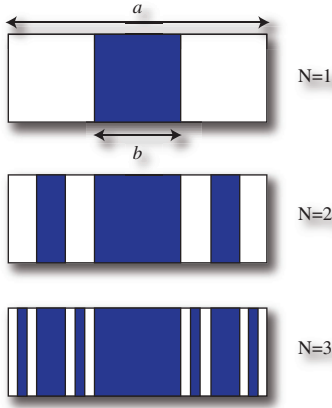


Fig. 1: (Color online) Pictorial representation of the generation of a Cantor-like 1D fractal photonic crystal.

step of the Cantor series depicted in fig. 1. We assume that the medium is stratified with interfaces normal to the z -axis, so that $\varepsilon = \varepsilon(z)$ and $\mu = \mu(z)$, and we take the plane of incidence to be the xz -plane. In the case of a TE field, it follows directly from the Maxwell equations that, for monochromatic waves of angular frequency ω , $\mathbf{E}(\mathbf{r}, t) = E(z) \exp[i(qx - \omega t)] \mathbf{e}_y$ and, for TM polarization, $\mathbf{H}(\mathbf{r}, t) = H(z) \exp[i(qx - \omega t)] \mathbf{e}_y$, where q is the wavevector component along the x -direction, and \mathbf{e}_y is the Cartesian unitary vector along the y -direction. The amplitudes of electric $E(z)$ and magnetic $H(z)$ fields satisfy the following ordinary differential equations:

$$\frac{d}{dz} \left[\frac{1}{\mu(z)} \frac{d}{dz} E(z) \right] = -\varepsilon(z) \left[\left(\frac{\omega}{c} \right)^2 - \frac{q^2}{n^2(z)} \right] E(z), \quad (1)$$

$$\frac{d}{dz} \left[\frac{1}{\varepsilon(z)} \frac{d}{dz} H(z) \right] = -\mu(z) \left[\left(\frac{\omega}{c} \right)^2 - \frac{q^2}{n^2(z)} \right] H(z), \quad (2)$$

where $n(z) = \sqrt{\varepsilon(z)} \sqrt{\mu(z)}$ is the z -dependent refractive index. In what follows, n_A and n_B are the refractive indices whereas ε_A (μ_A) and ε_B (μ_B) denote the dielectric permittivities (magnetic permeabilities) in layers A and B, respectively. We assume layers A of air ($\varepsilon_A = \mu_A = 1$), and layers B of a dispersive refractive-index metamaterial. In the B layers we consider a Drude-like model for both the electric and magnetic responses which, neglecting losses, may be written as $\varepsilon_B(\omega) = \varepsilon_0 - \frac{\omega_p^2}{\omega^2}$ and $\mu_B(\omega) = \mu_0 - \frac{\omega_m^2}{\omega^2}$, respectively. Here we choose $\varepsilon_0 = 1.21$ and $\mu_0 = 1.0$, as in previous work [15]. The electric and magnetic bulk (layer B) plasmon modes are at $\nu = \nu_e = \frac{\omega_e}{2\pi\sqrt{\varepsilon_0}}$ and $\nu = \nu_m = \frac{\omega_m}{2\pi\sqrt{\mu_0}}$, which correspond to the solutions of $\varepsilon_B(\omega) = 0$ and $\mu_B(\omega) = 0$, respectively. In the case of a TE electromagnetic wave, in order to solve eq. (1), we consider

the two-component function $\Psi(z) = \begin{pmatrix} E(z) \\ \frac{1}{\mu(z)} \frac{d}{dz} E(z) \end{pmatrix}$ which is continuous through the photonic structure, and write $\Psi(z_j) = \mathbf{M}_j(z_j - z_0) \Psi(z_0)$, where $\mathbf{M}_j(z_j - z_0)$ is the

corresponding transfer matrix. The transfer matrix for each layer of normal material A may be written as

$$\mathbf{A}_N = \begin{pmatrix} \cos(\kappa_{A,N}a) & \frac{\mu_A}{Q_A} \sin(\kappa_{A,N}a) \\ -\frac{Q_A}{\mu_A} \sin(\kappa_{A,N}a) & \cos(\kappa_{A,N}a) \end{pmatrix}, \quad (3)$$

where $\kappa_{A,N} = Q_A \left(\frac{1}{3}\right)^N$, and N corresponds to the respective Cantor step. For layers of metamaterial B, we have

$$\mathbf{B}_m = \begin{pmatrix} \cos(\kappa_{B,N}b) & \frac{\mu_B}{Q_B} \sin(\kappa_{B,N}b) \\ -\frac{Q_B}{\mu_B} \sin(\kappa_{B,N}b) & \cos(\kappa_{B,N}b) \end{pmatrix}, \quad (4)$$

where $\kappa_{B,N} = Q_B \left(\frac{1}{3}\right)^{N-1}$, with Q_A and Q_B as defined in ref. [9], and m varying from 1 to N . We denote as \mathbf{G}_N the transfer matrix obtained by the product $\mathbf{G}_N = \mathbf{A}_N \mathbf{B}_N \mathbf{A}_N$. For $N \geq 3$, the transfer matrix \mathbf{M}_N for a Cantor-like fractal photonic crystal (for $N = 1$ and $N = 2$, one obtains $\mathbf{M}_1 = \mathbf{G}_1 = \mathbf{A}_1 \mathbf{B}_1 \mathbf{A}_1$ and $\mathbf{M}_2 = \mathbf{G}_2 \mathbf{B}_1 \mathbf{G}_2$) may be expressed as

$$\mathbf{M}_N = \left(\left(\left(\left(\Gamma_{N,N-1,N-2}^{(3)} \mathbf{K}_N - \mathbf{B}_{N-2}^{-1} \right) \Gamma_{N,N-1,N-2,N-3}^{(4)} - \mathbf{B}_{N-3}^{-1} \right) \cdot \Gamma_{N,N-1,N-2,N-3,N-4}^{(5)} - \mathbf{B}_{N-4}^{-1} \right) \cdot \Gamma_{N,N-1,N-2,N-3,N-4,N-5}^{(6)} - \mathbf{B}_{N-5}^{-1} \right) \cdot \dots \right), \quad (5)$$

where

$$\mathbf{K}_N = \text{tr}(\mathbf{G}_N \mathbf{B}_{N-1}) \mathbf{G}_N - \mathbf{B}_{N-1}^{-1}, \quad (6)$$

and coefficients $\Gamma_{i_1, i_2, \dots, i_N}^{(N)}$ may be recursively obtained as

$$\Gamma_{i,j,k}^{(3)} = \text{tr}(\mathbf{G}_i \mathbf{B}_j) \text{tr}(\mathbf{G}_i \mathbf{B}_k) - \text{tr}(\mathbf{B}_j^{-1} \mathbf{B}_k), \quad (7)$$

$$\Gamma_{i,j,k,l}^{(4)} = \Gamma_{i,j,k}^{(3)} \Gamma_{i,j,l}^{(3)} - \text{tr}(\mathbf{B}_k^{-1} \mathbf{B}_l), \quad (8)$$

$$\Gamma_{i,j,k,l,m}^{(5)} = \Gamma_{i,j,k,l}^{(4)} \Gamma_{i,j,k,m}^{(4)} - \text{tr}(\mathbf{B}_l^{-1} \mathbf{B}_m), \quad (9)$$

$$\Gamma_{i,j,k,l,m,n}^{(6)} = \Gamma_{i,j,k,l,m}^{(5)} \Gamma_{i,j,k,l,n}^{(5)} - \text{tr}(\mathbf{B}_m^{-1} \mathbf{B}_n), \quad (10)$$

and so on. It is then straightforward to obtain the trace of the transfer matrix (5) for each step of the Cantor series. If we consider an unitary cell with length a , it is easy to see that the widths of layers A are determined by $\left(\frac{1}{3}\right)^N a$, and the total length of the unitary cell for each step of the Cantor series may be written as $L_N = \left(\frac{2}{3}\right)^N a + \sum_{j=0}^{N-1} \left(\frac{2}{3}\right)^j b$, where b is the length of the initial metamaterial layer B. One may then show that, if $b = \frac{a}{3}$, L_N is invariant, *i.e.*, $L_N = a$ for all N , as expected.

By imposing the periodicity constraint and using the Bloch condition [16], we obtain that the dispersion relation for each step N of the Cantor series may be written as

$$\cos(kL_N) = \frac{1}{2} \text{tr}(\mathbf{M}_N), \quad (11)$$

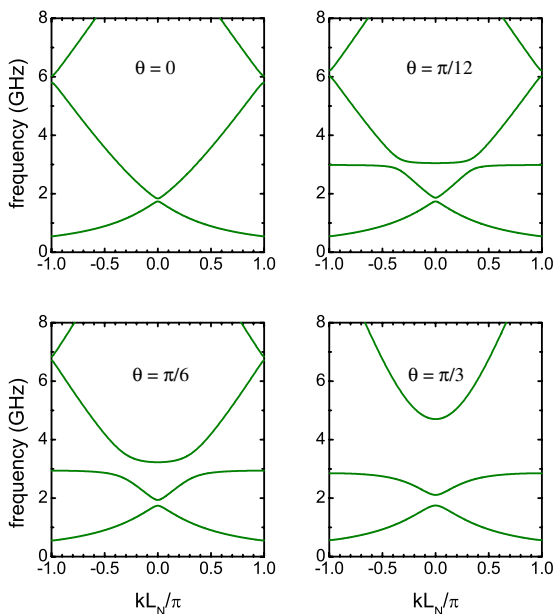


Fig. 2: (Color online) TE dispersion relations, $\nu = \nu(k)$, for a first-order $N = 1$ Cantor-like fractal photonic superlattice ($\nu = \frac{\omega}{2\pi}$), with $a = 27$ mm and $b = 9$ mm, for different incidence angles.

where k is the Bloch wave vector along the z -direction which is the axis of the photonic superlattice.

One should mention that calculations for the TM configuration may be essentially handled in the same way as detailed above for TE waves. Results here are presented for TE polarization and were obtained by using the above-mentioned Drude-like responses for slab B, with $\frac{\omega_p}{2\pi} = \frac{\omega_m}{2\pi} = 3$ GHz. Figure 2 presents the TE dispersion $\nu = \frac{\omega}{2\pi} = \nu(k)$ for a first step Cantor-like fractal photonic superlattice with $a = 27$ mm and $b = 9$ mm and different angles of incidence. As one would expect, for the $N = 1$ first step of the Cantor series, the photonic superlattice is a simple periodic photonic crystal composed by two alternating slabs of materials A and B. One may observe that, for $\theta \neq 0$, there is a non-Bragg $\langle n \rangle = 0$ gap and a non-Bragg plasmon-polariton gap, well discussed in previous work [9–11].

In fig. 3 we display the dispersion of TE electromagnetic waves, for normal incidence ($\theta = 0$), in photonic periodic superlattices with unit cells given by the $N = 1, 2$ and 3 steps of the Cantor series, respectively. We should mention that we are dealing with a Cantor-like photonic crystal with initial ($N = 1$ step) B layer width $b = a/3$, which leads to the unit cell width $L_N = a$, as mentioned above. As one increases the steps in the Cantor series, the proportion of normal A material within the unit cell diminishes, and the content $M_B = a[1 - (\frac{2}{3})^N]$ of metamaterial B increases, which explains the displacement of the $\langle n \rangle = 0$ gap, which tends to ν_m as expected, because its edges are located at $[\mu(\nu)] = 0$ and $[\varepsilon(\nu)] = 0$ and as $N \rightarrow \infty$, one obtains $\langle \mu(\nu) \rangle = \mu_B(\nu) = 0$ and $\langle \varepsilon(\nu) \rangle = \varepsilon_B(\nu) = 0$. On the other

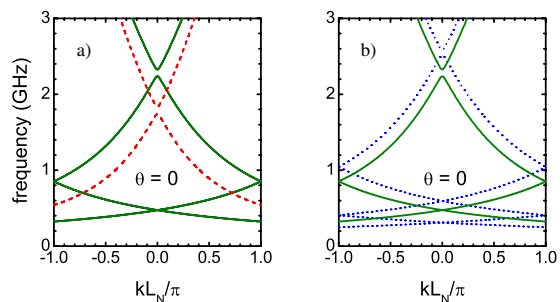


Fig. 3: (Color online) TE dispersion relations, $\nu = \nu(k)$, for normal incidence ($\theta = 0$) for Cantor-like fractal photonic superlattices with $a = 27$ mm and $b = 9$ mm. Dashed, solid and dotted lines correspond to 1st, 2nd and 3rd steps of the Cantor series, respectively.

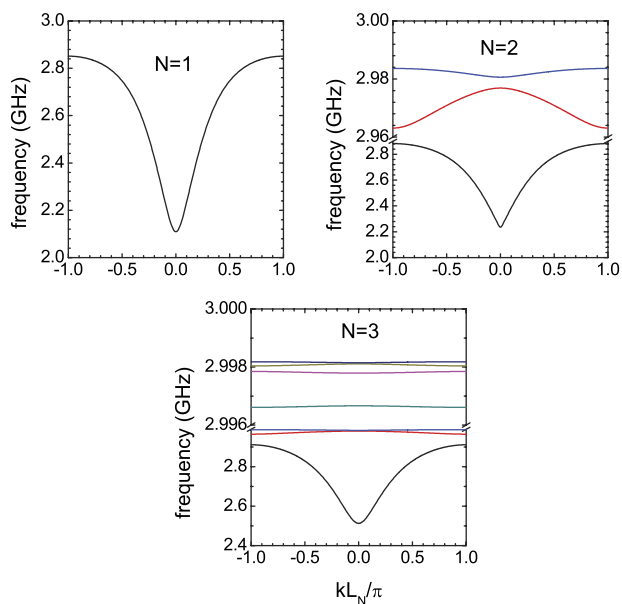


Fig. 4: (Color online) TE dispersion relations, $\nu = \nu(k)$, for Cantor-like fractal photonic superlattices with $a = 27$ mm and $b = 9$ mm, in the vicinity of the magnetic plasmon frequency $\nu_m = 3$ GHz, for various values of the Cantor step and incidence angle $\theta = \pi/3$. Note that the number of plasmon-polariton modes is $S_B = 2^N - 1$.

hand, one may notice that there is one $N = 1$ lower band below the $\langle n \rangle = 0$ gap, three subbands (for $N = 2$) with null gaps below the $\langle n \rangle = 0$ gap, and $J_N = 2^N - 1$ bands below the $\langle n \rangle = 0$ gap for a general N step of the Cantor series.

In order to study and characterize the plasmon-polariton modes in Cantor-like fractal photonic crystals, we display the TE dispersion $\nu = \nu(k)$ for the first three Cantor steps in fig. 4 around $\nu_m = 3$ GHz. If we denote $S_N = S_A^N + S_B^N$ as the number of slabs for each Cantor step, where S_A^N and S_B^N represent the number of slabs of materials A and B, respectively, one obtains that $S_A^N = 2^N$ and $S_B^N = 2^N - 1$. As one may see, the number of excited plasmon-polariton modes corresponds to the

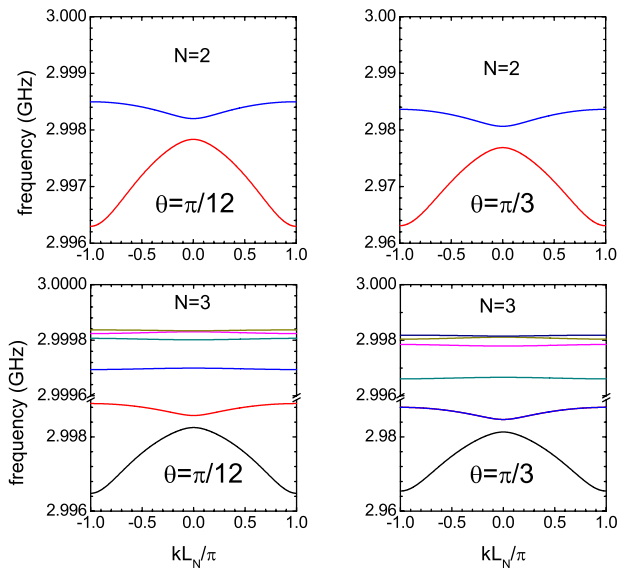


Fig. 5: (Color online) TE dispersion relations, $\nu = \nu(k)$, for plasmon-polariton modes in Cantor-like fractal photonic superlattices with $a = 27$ mm and $b = 9$ mm, for $N = 2$ and $N = 3$, with incidence angles $\theta = \pi/12$ and $\theta = \pi/3$.

number of metamaterial layers, $S_B^N = 2^N - 1$, in the unit cell of the Cantor-like photonic superlattice. From fig. 4, we notice that the single plasmon-polariton subband for $N = 1$ splits into $S_B^2 = 3$ for $N = 2$, and into $S_B^3 = 7$ for $N = 3$. Another important feature that we may observe in fig. 4 is that the dispersion of the successive plasmon-polariton bands is related to the widths of the layers of the metamaterial B. The plasmon-polariton band for $N = 1$ essentially remains the same as the lowest band in fig. 4 for $N = 2$, which is related to the central slab of metamaterial B, and the two thin bands for $N = 2$ are associated to the two new metamaterial slabs, and so on for higher steps of the Cantor series. In order to clarify the above discussion, in fig. 5 we magnify the higher plasmon-polariton bands for Cantor steps $N = 2$ and $N = 3$ ($a = 27$ mm, and $b = 9$ mm) and incidence angles $\theta = \pi/12$ and $\theta = \pi/3$. We may notice that some bands for $N = 2$ are also present in $N = 3$ and show the same behavior with θ . In fig. 6 we present the TE dispersion relations $\nu = \nu(k)$ for Cantor steps $N = 1$ and $N = 2$, for incidence angles $\theta = \pi/12$ and $\theta = \pi/3$, with $a = 27$ mm, and $b = 9$ mm. One observes that, for $N = 1$, the upper edge of the $\langle n \rangle = 0$ gap increases with increasing θ , whereas for $N = 2$ the reverse occurs. This behavior is due to the fact that the non-Bragg $\langle n \rangle = 0$ gap behavior clearly depends on the Cantor step, due to the increase of metamaterial content in the unit cell. One may stress that higher plasmon-polariton bands become essentially dispersionless as N increases. These plasmon-polariton bands are related to the narrow metamaterial layers located around the central slab B. The optical coupling between such slabs and its equivalent slabs in other unit cells of the periodic system is weaker than the

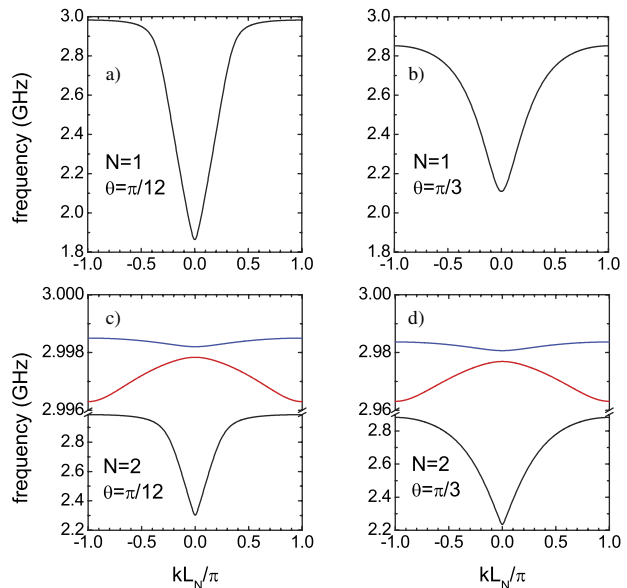


Fig. 6: (Color online) TE dispersion relations, $\nu = \nu(k)$, for plasmon-polariton modes in Cantor-like fractal photonic superlattices with $a = 27$ mm and $b = 9$ mm, for $N = 1$ and $N = 2$, with incidence angles $\theta = \pi/12$ and $\theta = \pi/3$.

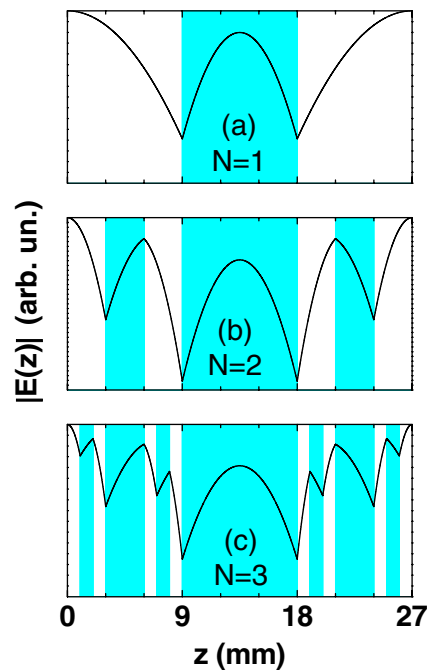


Fig. 7: (Color online) Electric field distribution along one period of the superlattice for $a = 27$ mm, $k = 0$, and $\theta = 0$, at the upper edge of the non-Bragg gap for $N = 1$, $N = 2$, and $N = 3$.

optical coupling between wider central slabs of different cells. As a consequence, the k -dependence of the group velocity associated to the plasmon-polariton subbands is weaker for higher subbands than for the lowest ones and, therefore, the higher plasmon-polariton subbands are basically nondispersive.

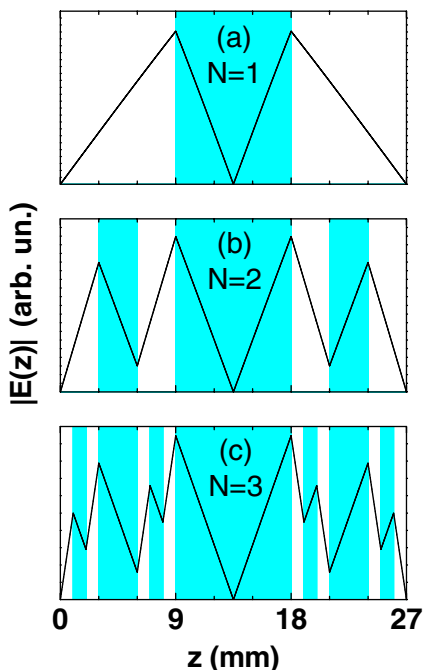


Fig. 8: (Color online) As in fig. 7, but for the lower edge of the non-Bragg gap.

In order to complete our study, we have computed the TE electric-field amplitude, as a function of the position in the elementary cell, in three different superlattices with the elementary cells corresponding to $N = 1$, $N = 2$ and $N = 3$. Numerical results, which were obtained for $a = 27$ mm and $\theta = 0$, are displayed in figs. 7 and 8 for $k = 0$ and frequencies at the higher and lower edges of the non-Bragg gap. The local behavior of the electric-field amplitude inside the elementary cell is determined by the slabs distribution in the system. One observes, therefore, a self-similar behavior of the electric-field amplitude as N increases.

Summing up, we have obtained the general transfer matrix and its trace for 1D Cantor-like fractal multilayer systems, and studied the plasmon-polariton modes in 1D Cantor-like fractal photonic superlattices composed of alternate layers of positive and dispersive left-handed materials. We have shown that the plasmon-polariton modes, which arise as a result of the coupling between photons and plasmons in such multilayered systems, strongly depend on the Cantor step N , and that the number $2^N - 1$ of plasmon-polariton bands, which show up for oblique incidence, corresponds to the number of metamaterial layers contained within the unit cell.

We would like to thank A. BRUNO-ALFONSO for useful discussions and suggestions. JRM-S would like to thank

M. SERRANO-MANTILLA for computing financial support. ER-G and LEO thank the Departamento de Física, Universidad del Valle, Cali, Colombia, for the warm hospitality, and ER-G also thanks the hospitality of the Instituto de Física, UNICAMP, where this work was completed. This research was partially supported by the Colombian Agency COLCIENCIAS, CODI - University of Antioquia, and Brazilian Agencies CNPq and FAPESP.

REFERENCES

- [1] VALENTINE J. *et al.*, *Nature*, **455** (2008) 376; XIAO S., DRACHEV V. P., KILDISHEV A. V., NI X., CHETTIAR U. K., YUAN H-K. and SHALAEV V. M., *Nature*, **466** (2010) 735 and references therein.
- [2] VESELAGO V. G., *Sov. Phys. Usp.*, **10** (1968) 509.
- [3] HOFFMAN A. J., ALEKSEYEV L., HOWARD S. S., FRANZ K. J., WASSERMAN D., PODOLSKIY V. A., NARIMANOV E. E., SIVCO D. L. and GMACHL C., *Nat. Mater.*, **6** (2007) 946.
- [4] LI J., ZHOU L., CHAN C. T. and SHENG P., *Phys. Rev. Lett.*, **90** (2003) 083901; DANINTE H., FOTEINOPOULOU S. and SOUKOULIS C. M., *Photon. Nanostruct. Fundam. Appl.*, **4** (2006) 123.
- [5] CAVALCANTI S. B., DE DIOS-LEYVA M., REYES-GÓMEZ E. and OLIVEIRA L. E., *Phys. Rev. E*, **75** (2007) 026607.
- [6] XIANG Y., DAI X. and WEN S., *J. Opt. Soc. Am. B*, **24** (2007) 2033; KOCAMAN S., CHATTERJEE R., PANOIU N. C., McMILLAN J. F., YU M. B., OSGOOD R. M., KWONG D. L. and WONG C. W., *Phys. Rev. Lett.*, **102** (2009) 203905.
- [7] BRUNO-ALFONSO A., REYES-GÓMEZ E., CAVALCANTI S. B. and OLIVEIRA L. E., *Phys. Rev. A*, **78** (2008) 035801.
- [8] LI J., ZHAO D. and LIU Z., *Phys. Lett. A*, **332** (2004) 461.
- [9] REYES-GÓMEZ E., MOGILEVTSEV D., CAVALCANTI S. B., DE CARVALHO C. A. A. and OLIVEIRA L. E., *EPL*, **88** (2009) 24002.
- [10] REYES-GÓMEZ E., RAIGOZA N., CAVALCANTI S. B., DE CARVALHO C. A. A. and OLIVEIRA L. E., *Phys. Rev. B*, **81** (2010) 153101.
- [11] DE CARVALHO C. A. A., CAVALCANTI S. B., REYES-GÓMEZ E. and OLIVEIRA L. E., *Phys. Rev. B*, **83** (2011) 081408(R).
- [12] LAVRINENKO A. V., ZHUKOVSKY S. V., SANDOMIRSKI K. S. and GAPONENKO S. V., *Phys. Rev. E*, **65** (2002) 036621; ZHUKOVSKY S. V., LAVRINENKO A. V. and GAPONENKO S. V., *Europhys. Lett.*, **66** (2004) 455.
- [13] XU P., TIAN H-P. and JI Y-F., *J. Opt. Soc. Am. B*, **27** (2010) 640.
- [14] FEDER J., *Fractals* (Plenum Press, New York) 1988.
- [15] JIANG H., CHEN H., LI H., ZHANG Y. and ZHU S., *Appl. Phys. Lett.*, **83** (2003) 5386.
- [16] BUSCH K., CHAN C. T. and SOUKOULIS C. M., in *Photonic Band Gap Materials*, edited by SOUKOULIS C. M. (Kluwer, Dordrecht) 1996.